Clays and Clay Minerals, Vol. 53, No. 1, 18–27, 2005.

SUBSTITUTION OF Fe^{3+} FOR Al^{3+} CATIONS IN LAYERED DOUBLE HYDROXIDE $[LiAl_2(OH)_6]_2CO_3{\cdot}nH_2O$

PIOTR KUŚTROWSKI*, AGNIESZKA WĘGRZYN, ALICJA RAFALSKA-ŁASOCHA, AGNIESZKA PATTEK-JANCZYK AND ROMAN DZIEMBAJ

Faculty of Chemistry, Jagiellonian University, Ingardena 3, 30-060 Kraków, Poland

Abstract—Synthesis of the Li-Al-Fe layered double hydroxides was performed by the coprecipitation method at constant pH (11.0±0.2) and temperature (40±2°C). Structural features of the as-synthesized samples were investigated by X-ray diffraction (XRD), infrared (IR) spectroscopy, scanning electron microscopy and Mössbauer spectroscopy. The samples consisted of well crystallized $[LiFe_xAl_{2-x}(OH)_6]_2CO_3{\cdot}nH_2O$ phases with strict ordering of M^+ and M^{3+} cations in the sheets. However, only a proportion of Al^{3+} could be substituted by Fe^{3+} ions. The excess Fe^{3+} cations formed a separate ferrihydrite phase. Incorporation of Fe into the hydrotalcite-like structure resulted in an increase in the *a* lattice parameter determined by XRD. In addition, a shift of IR absorption bands, ascribed to the stretching vibrations of interlayer CO_3^{2-} anions as well as the transitional motions of oxygen in the layers, to lower frequencies was observed. The presence of Fe^{3+} in the octahedral sheets caused a splitting of the band assigned to the stretching vibrations of the layer OH groups. Mössbauer experiments revealed that Fe exists in the synthesized samples in two different chemical environments. A proportion of the Fe^{3+} cations is incorporated as isolated ions in the $[LiFe_xAl_{2-x}(OH)_6]_2CO_3{\cdot}nH_2O$ crystal structure. However, Fe^{3+} ions forming the ferrihydrite phase are dominant in the Fe-rich materials.

Key Words—FTIR, Hydrotalcite-like Compounds, Li-Al-Fe Layered Double Hydroxides, Mössbauer Spectroscopy, SEM, XRD.

INTRODUCTION

Hydrotalcite-like compounds are layered double hydroxides (LDHs) with the general formula $[M^{z+}_{1-x}M^{3+}_x(OH)_2]^{A+}X^{m-}_{A/m}{\cdot}nH_2O$, where $A = x$ for $z = 2$ and $A = 2x-1$ for $z = 1$ (Cavani *et al.*, 1991). The possibility of synthesizing LDHs which contain monovalent cations is limited to Li^+ ions only. As monovalent cations present in $[LiAl_2(OH)_6]^+X^-$ fill the octahedral vacancies between Al ions arranged as in gibbsite (Serna *et al.*, 1982), Na^+ and other monovalent cations are too large to occupy these vacancies (Sissoko *et al.*, 1985). The fact that $[LiAl_2(OH)_6]^+X^-$ are $Al(OH)_3$-derived compounds was proved by XRD studies which showed that cations are largely ordered in the Li compound in contrast to M^{2+}/M^{3+} LDHs possessing a general tendency towards cation disorder. The presence of Li^+ in the free octahedral sites of gibbsite-like sheets results in an appearance of positive charge which is counterbalanced by the interlayer anions (X^-).

The ion-exchanging ability of Li aluminate hydroxide system has been widely studied. To modify the properties of $[LiAl_2(OH)_6]^+X^-$ a great number of different anions was introduced into the interlayer, *e.g.* NO_3^-, Cl^-, $V_2O_7^{4-}$, $V_{10}O_{28}^{6-}$, long chain (>C_{10}) fatty acids (Chisem and Jones, 1994; Twu and Dutta, 1989; Dutta and Robins, 1994). No successful efforts at synthesizing LDHs combining Li^+ with other than Al^{3+} cations have been described. Nevertheless, $[LiM^{III}_2(OH)_6]^+X^-$ containing Cr^{3+}, Fe^{3+}, Ga^{3+} and In^{3+} can be imagined (Rajamathi *et al.*, 2001). Incorporation of a transition metal into the I-III LDHs would make these materials attractive as potential catalyst precursors or catalysts.

The purpose of this work was to incorporate Fe^{3+} into $[LiAl_2(OH)_6]_2CO_3{\cdot}nH_2O$ and this aim was achieved. We prepared materials with different Fe contents and determined their structural features by XRD and spectroscopic methods.

EXPERIMENTAL

Preparation of samples

$[LiAl_2(OH)_6]_2CO_3{\cdot}nH_2O$ (sample denoted Fe0) was prepared by coprecipitation at low supersaturation and constant pH (11.0±0.2) and temperature (40°C±2°C). Both, $LiNO_3{\cdot}3H_2O$ (0.10 mole) and $Al(NO_3)_3{\cdot}9H_2O$ (0.10 mole) were mixed and dissolved in 400 ml of distilled water. The solutions of nitrates and 10 wt.% NaOH (used as pH-controlling agent) were simultaneously added dropwise to the aqueous solution of Na_2CO_3 (0.06 mole) under vigorous stirring. The pH of the sodium carbonate solution had been previously adjusted to 11.0 by the addition of concentrated HNO_3. During the synthesis, special attention was paid to maintaining pH and temperature within the intended range. The precipitate obtained was left overnight under gentle stirring for further crystallization, then filtered

* E-mail address of corresponding author:
kustrows@chemia.uj.edu.pl
DOI: 10.1346/CCMN.2005.0530103

Copyright © 2005, The Clay Minerals Society

https://doi.org/10.1346/CCMN.2005.0530103 Published online by Cambridge University Press

and washed several times to remove nitrate residues. The sample was then dried for 12 h at 120ºC in air.

In the following syntheses, Al^{3+} ions were progressively replaced by Fe^{3+} cations using appropriate amounts of $Fe(NO)_3 \cdot 9H_2O$ instead of aluminum nitrate. First, 5 atom.% of Al was exchanged in the mother solution, then 15, 30, 45, 60 and 100 atom.% and the samples were denoted Fe5, Fe15, Fe30, Fe45, Fe60 and Fe100, respectively.

Samples denoted Fe′5, Fe′30 and Fe′60 were prepared as reference materials with no addition of lithium nitrate during coprecipitation using the method described above.

Characterization techniques

Powder XRD patterns were obtained using a PW3710 Philips X'pert diffractometer using Ni-filtered CuKα radiation (λ = 1.54178 Å) over a 2θ range of 4 to 80º (step size – 0.025º, time per step – 1.5 s). Fourier transform infrared (FTIR) spectra were recorded from 400 to 4000 cm^{-1} with a Bruker IFS 48 spectrophotometer using the KBr pellet technique. Directly before the FTIR experiments, the synthesized materials were additionally dried at 100ºC for 3 h. Scanning electron micrographs were obtained using a PHILIPS XL 30 scanning electron microscope equipped with a LINK-ISIS EDX system. The total Fe and Al content in the samples was determined by XRF (Oxford 2000) spectrometer.

Mössbauer spectra of the as-synthesized samples were recorded at room temperature using a conventional spectrometer with a $^{57}Co(Rh)$ source. Additional measurements at low temperature (15 K) were performed for the Fe5 and Fe30 samples. For γ-ray detection a Kr-filled proportional counter was applied. The samples were powdered and pressed into pellets, their effective thickness being ~7–10 mg Fe/cm^2. The spectra were analyzed numerically by means of a linear least-squares procedure assuming Lorentzian shape of the absorption lines. The isomer shift values were calculated with respect to α-Fe at room temperature.

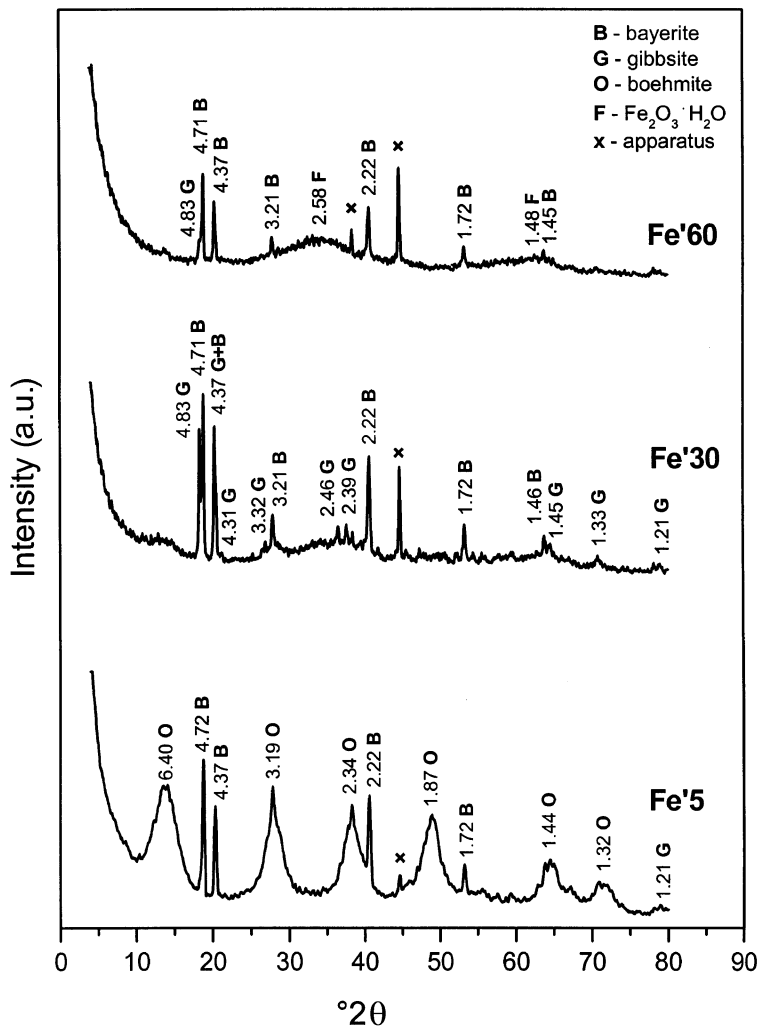

Figure 1. XRD patterns of Al-Fe samples.

https://doi.org/10.1346/CCMN.2005.0530103 Published online by Cambridge University Press

RESULTS AND DISCUSSION

X-ray diffraction

The XRD patterns of the samples which do not contain Li (Figure 1) show that coprecipitation from the aqueous Al and Fe nitrates solution at strong basic conditions (pH = 11.0) leads to the formation of mixtures of (oxo)hydroxide phases: boehmite, bayerite and/or gibbsite (Ramos Gallardo and Vegas, 1996). The poorly crystallized boehmite phase is dominant for the Fe'5 sample containing the smallest amount of Fe. The X-ray reflections characteristic for bayerite are also present in the XRD pattern of this solid. An increase in the Fe content results in the disappearance of the boehmite phase and the formation of a mixture of bayerite and gibbsite structures. The very broad and weak diffraction lines observed for the Fe'60 sample at ~2.61 and 1.49 Å suggest the presence of an almost X-ray amorphous 2-line ferrihydrite phase (Schwertmann and Cornell, 1991).

The results of XRD analysis for the Fe0 sample, which was prepared by the same synthesis procedure, but using Li and Al nitrate solutions, are presented in Figure 2. The XRD pattern of this sample is typical of that for $[LiAl_2(OH)_6]_2CO_3{\cdot}nH_2O$ (Serna *et al.*, 1982). The reflection at $d = 4.37$ Å distinguishes this XRD pattern from others characteristic of hydrotalcite-like compounds (Miyata, 1975). The appearance of this diffraction feature, indexed as 101 in a (pseudo)hexagonal unit-cell, can be explained by the strict ordering of Li^+ and Al^{3+} cations in the sheets of $[LiAl_2(OH)_6]_2CO_3{\cdot}nH_2O$ (Taylor, 1969). The shape of this maximum indicates, however, an existence of turbostratic crystals which means that the layers are stacked along the normal to d_{001} so that no layer is tilted with respect to that line. The layers are displaced from each other in the *X-Y* plane by random shifts and are rotated about the normal by random angles. No residual reflections corresponding to Al (oxo)hydroxides are evident, indicating that Al is completely incorporated within the LDH structure. The lattice parameters of the synthesized $[LiAl_2(OH)_6]_2CO_3{\cdot}nH_2O$ material calculated using the PROSZKI system (Łasocha and Lewiński,

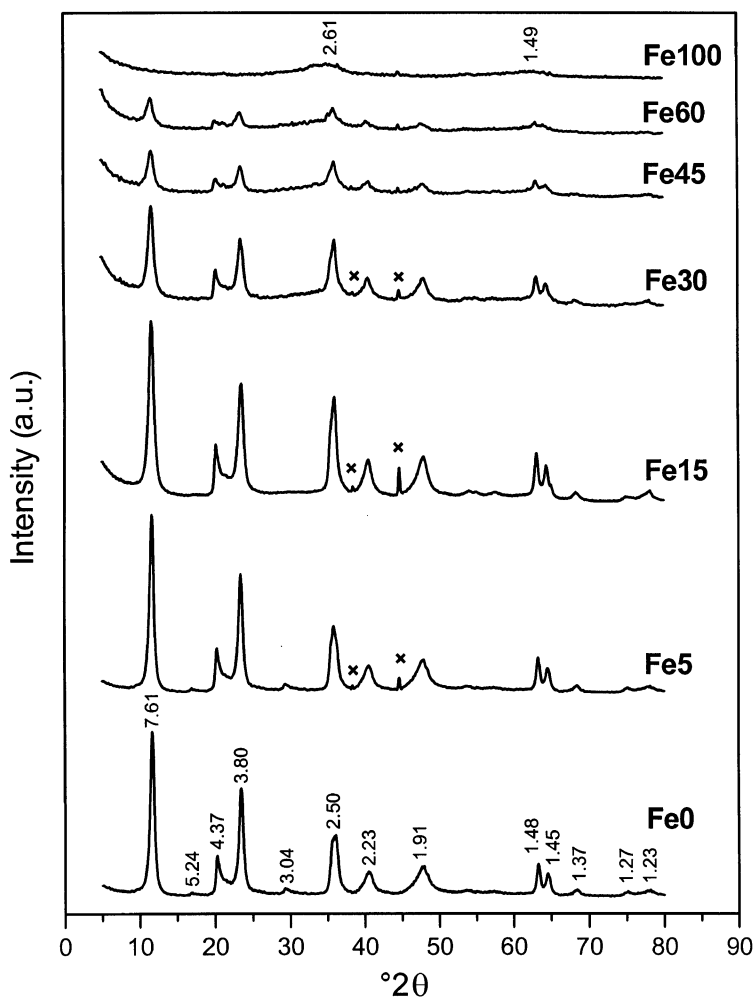

Figure 2. XRD patterns of Li-doped Al-Fe samples.

https://doi.org/10.1346/CCMN.2005.0530103 Published online by Cambridge University Press

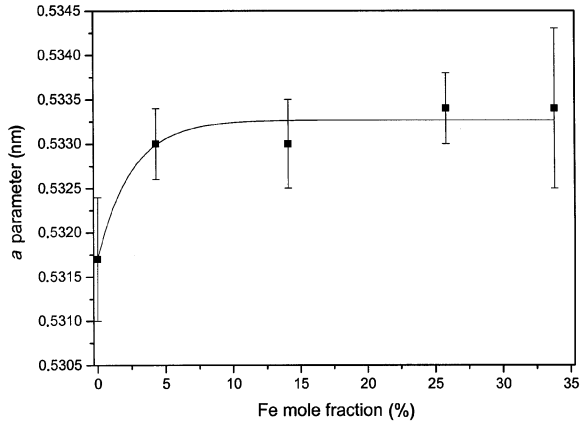

Figure 3. Effect of Fe content in the sample (determined by XRF analysis) on the value of the *a* lattice parameter of LDHs.

1994) are as follows: a = 5.317(7) Å and c = 15.19(2) Å (e.o.f. = 0.90). The crystallite size was calculated based on the Scherrer equation which was derived from the Bragg Law (Klug and Alexander, 1974):

$$\beta = K\lambda/T\cos\theta$$

According to these calculations (based on 002 and 004 reflections) the crystallite size for the Fe0 sample is equal to 100 Å.

The XRD patterns of the samples with a partial substitution of Fe^{3+} for Al^{3+}, as shown in Figure 2, do not differ significantly from that of Fe0. Thus, it should be pointed out that coprecipitation of mixed Li, Al and Fe hydroxides results in the appearance of an LDH structure unlike those of the Al-Fe samples which form mixtures of (oxo)hydroxides phases. The lattice parameters of the Fe,Al-rich samples are as follows: a = 5.330(4) Å and c = 15.24(1) Å (e.o.f. = 0.68) for Fe5, a = 5.330(5) Å and c = 15.22(1) Å (e.o.f. = 0.62) for Fe15, a = 5.334(4) Å and c = 15.23(1) Å (e.o.f. = 0.50) for Fe30 and a = 5.334(9) Å and c = 15.23(2) Å (e.o.f. = 1.09) for Fe45. The changes in the value of the a parameter as a function of the percentage of Al atoms exchanged by Fe (determined by X-ray fluorescence (XRF) analysis of bulk composition of the samples) are presented in Figure 3. The value of the a parameter increases with the introduction of a small fraction of Fe to the sample. Incorporating more Fe does not cause noticeable changes in the measured values of the a lattice parameter. On the other hand, the

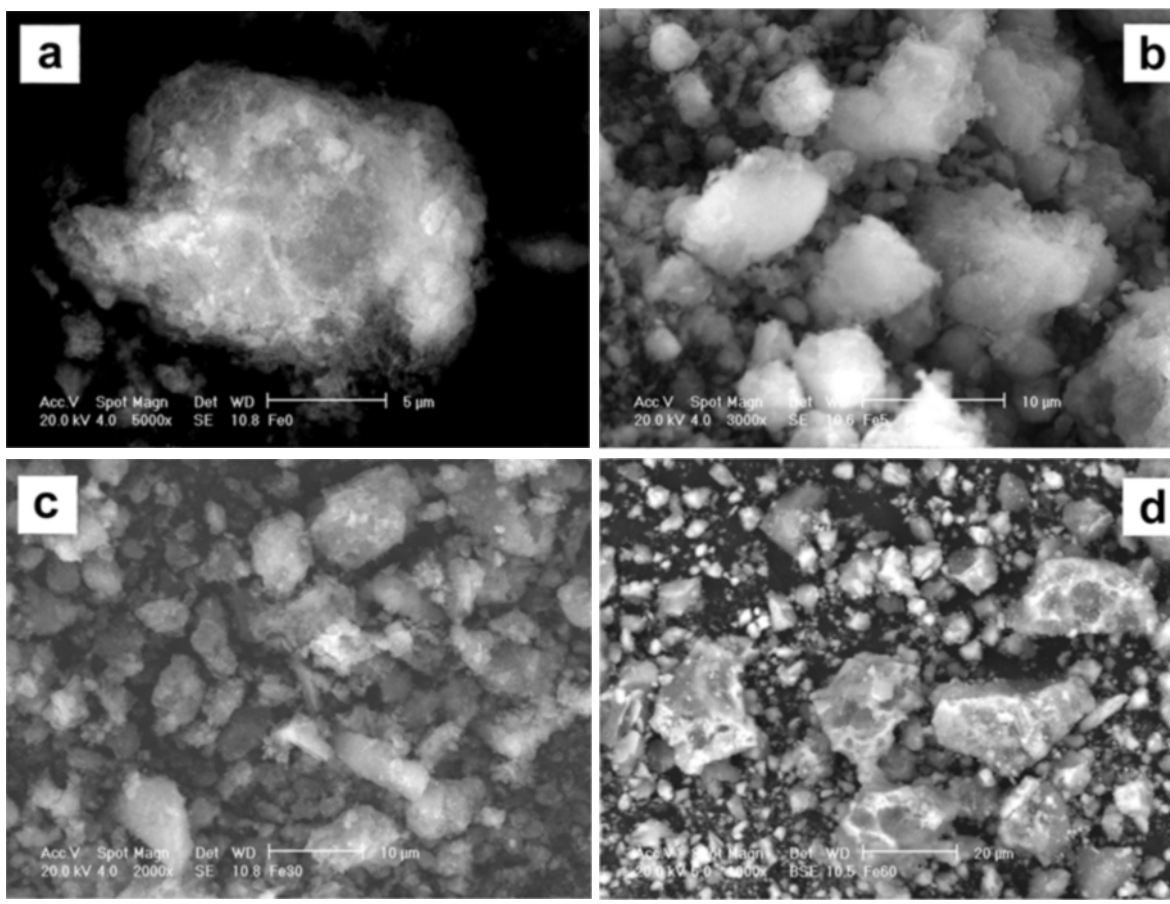

Figure 4. SEM images of Fe0 (a), Fe5 (b), Fe30 (c) and Fe60 (d) samples.

https://doi.org/10.1346/CCMN.2005.0530103 Published online by Cambridge University Press

peculiar reflection at d = 4.37 Å is still present in the XRD patterns of Fe,Al-rich samples strongly suggesting an ordering of M^{+}/M^{3+} cations amongst the octahedral sheets. Thus, Fe^{3+} cations were probably incorporated in the LDH structure by occupying positions of Al^{3+} in the $[LiAl_2(OH)_6]^{+}$ sheets. However, the amount of Fe which can be introduced into the LDH structure is limited. Moreover, the crystallinity of the materials decreases with increasing Fe content. The mean crystallite sizes of the samples studied are as follows: 97 Å (for Fe5), 80 Å (for Fe15), 77 Å (for Fe30) and 73 Å (for Fe45). In the XRD pattern of the Fe45 sample, very broad and weak reflections at ~2.61 and 1.49 Å, which can be attributed to the ferrihydrite structure, appear. These diffraction lines become more distinct for Fe60. In the case of the almost totally amorphous Fe100 sample, ferrihydrite is the only phase. It should be noted that the possible presence of ferrihydrite (in amounts below detection by XRD) in the samples with low Fe content cannot be excluded.

Scanning electron micrographs and X-ray microanalysis

The scanning electron microscope (SEM) images (Figure 4) indicate that all the samples, constituted by

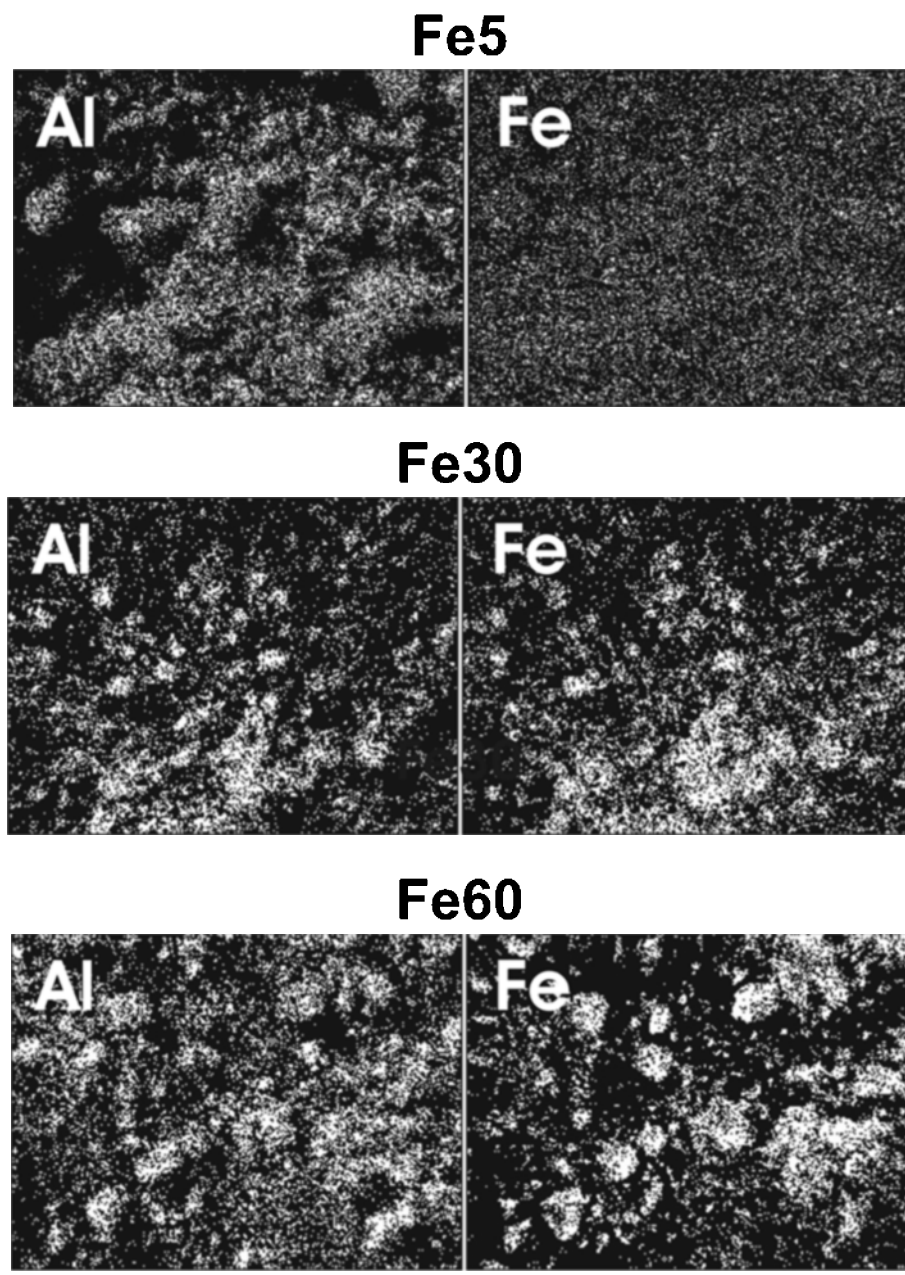

Figure 5. Mappings of Al and Fe distribution on surfaces of the Fe5, Fe30 and Fe60 samples.

https://doi.org/10.1346/CCMN.2005.0530103 Published online by Cambridge University Press

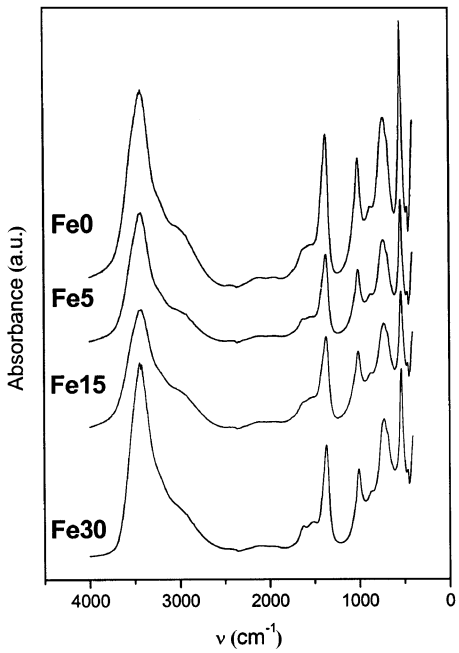

Figure 6. FTIR spectra of the dried samples from 4000 to 400 cm^{-1}.

agglomerates of compact, non-porous grains, are poorly crystalline. Moreover, it should be noted that the particle size decreases with an increase of the Fe content in the sample which is consistent with the XRD patterns. The X-ray mappings (Figure 5) show that Fe and Al are distributed uniformly in the samples studied. However, slight differences in the arrangement of Fe and Al were observed at each Fe content.

Infrared spectroscopy

The infrared (IR) spectra for the dried samples, which did not show distinct diffraction lines attributable to a ferrihydrite phase, were recorded at room temperature. The results obtained are presented in Figure 6. All the studied materials show bands of typical carbonate-containing hydrotalcite-like compound. The band positions with proper assignment of the samples are summarized in Table 1.

The H-bonding-stretching and bending vibrations of OH groups in the layers can be identified at 3425–3447 cm^{-1} and 1008–1010 cm^{-1}, respectively. In the OH-stretching region of the samples containing Fe, two bands (centered at ~3447 cm^{-1} and 3425 cm^{-1}) can be identified. This can be attributed to the difference in the electron density around the OH group, which is affected by the polarizability of the trivalent cations – Al^{3+} and Fe^{3+} (Kannan and Swamy, 1997). A very similar position of the band assigned to the stretching of OH groups coordinated by Fe atoms (3432–3474 cm^{-1}, depending on the Fe content in hydrotalcite) was found previously (Hansen and Koch, 1995). The bending mode of interlayer and/or adsorbed water appears at ~1630 cm^{-1}.

The positive charge of $[LiFe_xAl_{2-x}(OH)_6]^+$ sheets is compensated by carbonate anions present in the interlayer space. The absorption bands characteristic of CO_3^{2-} ions are found at frequencies of 1366 cm^{-1} (ν_3), 870 cm^{-1} (ν_2) and 688 cm^{-1} (ν_4) for the Fe0 sample. A substitution of Al by Fe and an increase in the Fe content result in a slight shift of peak positions to 1365 cm^{-1}, 866–868 cm^{-1} and 686–687 cm^{-1}. It is most likely that an excess of Fe localized in the OH sheets of material causes lowering of symmetry of the carbonate species due to stronger interaction between CO_3^{2-} anions and the layers of LDH. Formation of H bonding between carbonates and water in the interlayer is proven by the presence of the CO_3^{2-}–H_2O bridging mode observed around 3000 cm^{-1} for all the samples investigated.

The absorption bands observed in the region of spectra below 800 cm^{-1} (Figure 7) can be assigned to transitional motions of the oxygen in the layers (Hernandez-Moreno *et al.*, 1985). Assumption of the ideal D_{3d} symmetry allows us to predict the presence of seven IR active modes: $3A_{2u}$ (M–O motions in the z direction) and $4E_u$ (M–O motions in the x and y directions). However, in the range of frequency studied, only three vibrations of M^{3+}–O are observed. The others should be located below 400 cm^{-1}. For the Fe0 sample, the Al–O motions appear at 728 cm^{-1} (A_{2u}), 539 cm^{-1} (E_u) and 463 cm^{-1} (E_u). The substitution of Al^{3+} by Fe^{3+} cations results in a gradual shift of lattice vibration positions to the lower frequencies (722 cm^{-1}, 533 cm^{-1} and 459 cm^{-1} for Fe30). It is noticed that the observed bands overlap partially with those characteristic for ferrihydrite (cf. Figure 7). The impact of ferrihydrite bands on the LDH spectra, however, is minimal. The A_{2u} band would be expected to shift to a lower wavenumber as the ferrihydrite content increased whereas the E_u

Table 1. IR band assignments of the studied hydrotalcites.

Sample	Hydroxyl vibrations (cm^{-1})		CO_3^{2-} vibrations (cm^{-1})			Lattice vibrations (cm^{-1})		
	ν_{OH} (str)	ν_{OH} (bend)	ν_2	ν_3	ν_4	M^{3+}–O (A_{2u})	M^{3+}–O (E_u)	M^{3+}–O (E_u)
Fe30	3430	1010	870	1366	688	728	539	463
Fe5	3446 + 3427	1010	870	1366	687	727	536	461
Fe15	3447 + 3425	1010	868	1365	687	722	533	459
Fe30	3447 + 3425	1008	866	1365	686	722	533	459

https://doi.org/10.1346/CCMN.2005.0530103 Published online by Cambridge University Press

bands would be expected to shift to a higher wavenumber. The changes in the A_{2u} and E_u peak positions as a function of the measured Fe mole fraction are illustrated in Figure 8. It is found that for Fe0 to Fe15 at least, all bands shift in the same direction (*i.e.* to lower wavenumbers) suggesting a systematic incorporation of Fe into the LDH structure. A non-linear relationship between the peak positions and the Fe content was found. Thus, the results obtained are essentially consistent with the XRD data, which showed that only limited substitution of Fe^{3+} into the $M^{3+}O_6$ groups of $[LiFe_xAl_{2-x}(OH)_6]^+$ sheets is possible.

Mössbauer experiments

All the room-temperature Mössbauer spectra of samples Fe5, Fe15 and Fe30 (Figure 9) reveal a similar shape, a slightly asymmetric doublet, and are similar to previously published Mössbauer data of hydrotalcite-like materials (Kumbhar *et al.*, 2000; Koch, 1998). One-doublet fits, computed as a first approximation to obtain the rough Mössbauer parameters, were of relatively poor quality, so the two Lorentzian doublets of different quadrupole splittings had to be considered. Nevertheless,

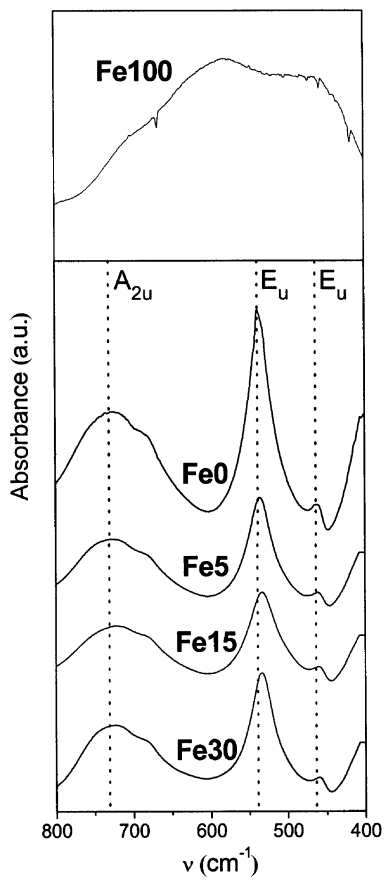

Figure 7. Comparison of the low-frequency region (400–800 cm^{-1}) of FTIR spectra of the ferrihydrite (Fe100) and LDH- (Fe0, Fe5, Fe15 and Fe30) containing samples.

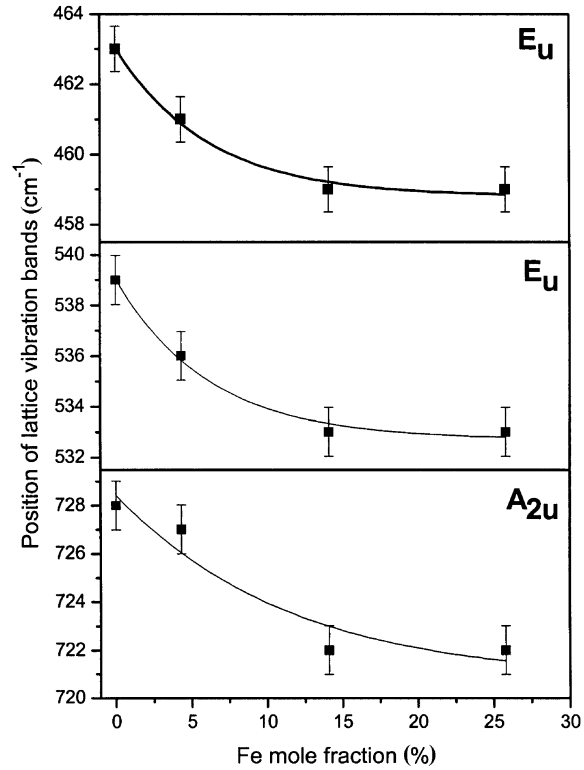

Figure 8. Changes in the A_{2u} and E_u peak position as the Fe content in the LDH-based samples is increased.

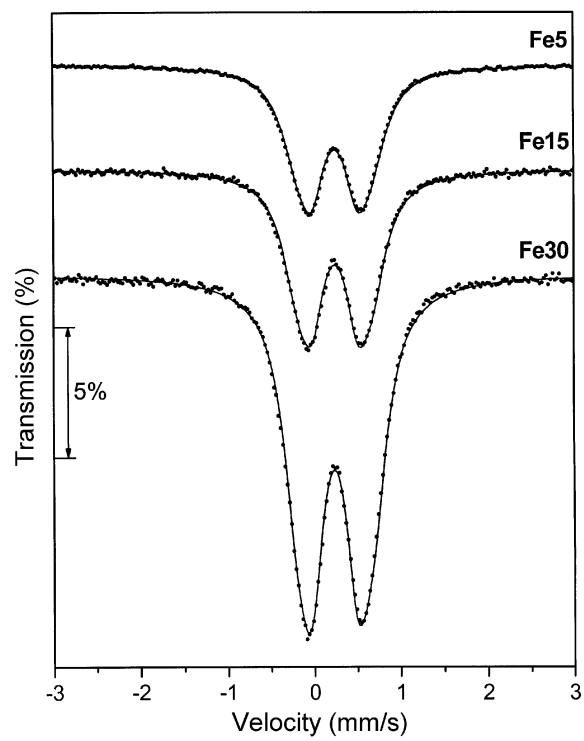

Figure 9. Mössbauer spectra of the samples fitted to two Lorentzian doublets.

https://doi.org/10.1346/CCMN.2005.0530103 Published online by Cambridge University Press

Table 2. Mössbauer data for the Li-Fe-Al samples fitted with different models.

Sample	Model	IS (mm/s)	QS (mm/s)	FWHM (mm/s)	Area (%)	χ^2
Fe5	One doublet	0.35(1)	0.66(1)	0.48(2)	100	6.55
	Two doublets	0.35(1)	0.52(1)	0.36(1)	49.5±3.2	2.65
		0.35(1)	0.85(1)	0.45(1)	50.5±3.4	
	Two doublet distribution	0.350(4)	0.59(20)		69.0	2.07
		0.357(7)	0.94(36)		31.0	
Fe15	One dublet	0.35(1)	0.67(1)	0.46(1)	100	3.21
	Two doublets	0.35(1)	0.53(1)	0.34(1)	51.5±4.5	1.51
		0.35(1)	0.87(2)	0.42(1)	48.5±4.7	
	Two doublet distribution	0.347(3)	0.57(17)		61.9	1.35
		0.353(5)	0.89(28)		38.2	
Fe30	One doublet	0.34(1)	0.67(1)	0.46(2)	100	7.60
	Two doublets	0.34(1)	0.54(1)	0.36(1)	55.7±2.4	2.28
		0.35(1)	0.89(1)	0.40(1)	44.3±2.5	
	Two doublet distribution	0.339(3)	0.56(18)		54.0	1.23
		0.345(5)	0.86(28)		46.0	

the best fits were obtained by taking into account the continuous distribution of quadrupole splittings. The application of simple linear correlation between the isomer shift and quadrupole splitting improved the fitting and resulted in the lowering of the χ^2 values. The Mössbauer parameters determined according to those three models are compiled in Table 2 where the χ^2 values are also included. The results obtained by means of the third model show the maximum of quadrupole splitting distributions and sigma values are presented in brackets. Regardless of the model used, the isomer shift values did not change significantly among samples or doublets. In contrast, the doublets differed from each other significantly in the quadrupole-splitting maxima and the distribution widths.

In Figure 10 the spectra fitted by the third model are presented and the quadrupole splitting distributions are inserted. Comparison of the distributions' probability reveals that in the Fe5 sample some asymmetry is visible. The distribution with the maximum at ~0.55 mm/s dominates significantly but the second component obviously exists. This asymmetry is less distinct when the higher Fe ion contents are introduced to the samples.

The results of XRD and IR studies suggest that in the Fe5, Fe15 and Fe30 samples, Fe was partially incorporated into the hydrotalcite structure. The changes of the Mössbauer parameters determined on the basis of room-temperature spectra are too small to confirm this suggestion explicitly. Thus, the Mössbauer spectra of the Fe5 and Fe30 samples (Figure 11) were recorded at a temperature of 15 K. They reveal a doublet in the middle part of the spectrum and a sextet, with a distribution of magnetic hyperfine fields, that is a dominant component in the spectrum. A similar sextet but in much smaller amount was found by Koch (1998) in the spectrum of natural, gold-colored pyroaurite and was attributed to the presence of Fe oxide in the sample. However, the average hyperfine field B_{hf} determined by Koch for the pyroaurite-like sample was equal to ~51 T in the spectrum taken at 12 K. For the samples studied in the present work the average B_{hf} was equal to ~40 T for Fe5 and ~46 T for Fe30, which are much lower than the value mentioned above. This behavior by Fe may be explained in two ways: either Fe^{3+} ions are located in neighboring sites within the hydrotalcite sheets forming the cluster-type arrangement or they create the separate phase of ferrihydrite. The XRD and FTIR data collected

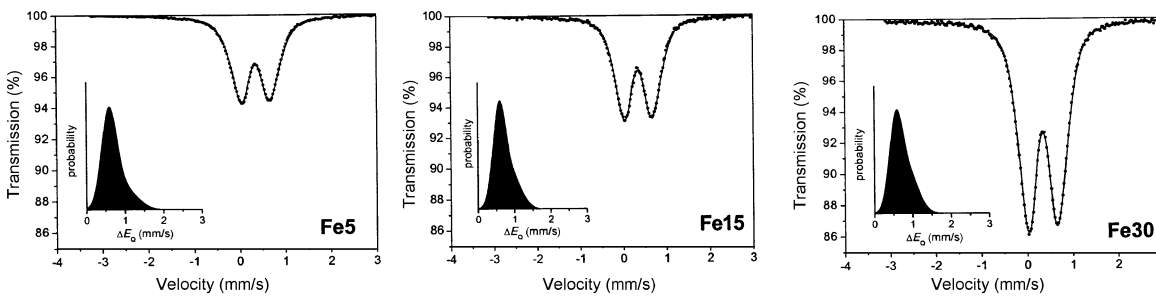

Figure 10. Mössbauer spectra of the Fe5, Fe15 and Fe30 samples fitted using a model of linear correlation between the isomer shift and the quadrupole splitting. The determined distributions of quadrupole splittings are also shown.

https://doi.org/10.1346/CCMN.2005.0530103 Published online by Cambridge University Press

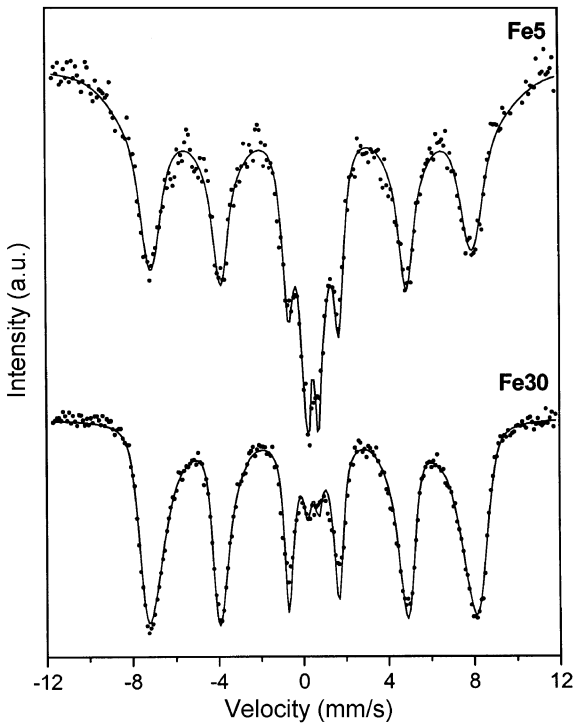

Figure 11. Mössbauer spectra of the Fe5 and Fe30 samples measured at 15 K.

suggest that an increase in the ferrihydrite content rather than Fe clustering is the dominant phenomenon.

CONCLUSIONS

Possible replacement of Al^{3+} by Fe^{3+} cations in the structure of layered double hydroxide $[LiFe_xAl_{2-x}(OH)_6]_2CO_3{\cdot}nH_2O$ was proven. Such hydrotalcites can be prepared by the coprecipitation method at constant temperature (40±2°C) and pH value (11.0±0.2). However, the amount of Fe cations incorporated in Li-Al LDHs is limited only to a few molar percent. The excess Fe used in the synthesis leads to the formation of the additional phase of ferrihydrite.

The Fe^{3+} cations substituted are situated in the Al^{3+} positions within the $[LiAl_2(OH)_6]^+$ sheets. The substitution does not change the strict ordering of M^+ and M^{3+} cations and the characteristic reflection at d = 4.37 Å is still observed in the XRD pattern. The shifts in the absorption band positions are observed for the Fe-rich samples in the FTIR spectra. The stretching vibrations of the interlayer CO_3^{2-} anions as well as the transitional motions of oxygen in the sheets can be found at lower frequencies in the FTIR spectra of the Li-Fe-Al samples than those for the $[LiAl_2(OH)_6]_2CO_3{\cdot}nH_2O$ precursor. Moreover, for the Fe-rich samples, the band assigned to the stretching vibrations of the OH groups in the sheets is split due to differences in the polarizability of Al^{3+} and Fe^{3+} cations. Mössbauer-effect measurements show that only a proportion of the Fe is situated as isolated Fe^{3+} cations in the $[LiAl_2(OH)_6]^+$ sheets. A majority of Fe^{3+} is present in the samples as the separate phase of ferrihydrite. Because of this, magnetic ordering of Fe^{3+} ions at low temperature (15 K) is observed.

ACKNOWLEDGMENTS

The authors would like to thank Jan Żukrowski from the Department of Physics, Academy of Mining and Metallurgy, Kraków, Poland, for performing Mössbauer measurements at 15 K. We are also grateful to Elżbieta Bielańska from the Aleksander Krupkowski Institute of Metallurgy and Materials Science of the Polish Academy of Sciences for taking the SEM pictures and to the Polish Committee of Scientific Research for financial support of this work (Grant No. PBZ/KBN/018/T09/99/3a).

REFERENCES

Cavani, F., Trifirò, F. and Vaccari, A. (1991) Hydrotalcite-type anionic clays: preparation, properties and application. *Catalysis Today*, **11**, 173–301.

Chisem, I.C. and Jones, W. (1994) Ion-exchange properties of lithium aluminum layered double hydroxides. *Journal of Materials Chemistry*, **4**, 1737–1744.

Dutta, P.K. and Robins, D.S. (1994) Interlayer dynamics of a fatty acid exchanged lithium aluminum layered double hydroxide monitored by infrared spectroscopy and pyrene fluorescence. *Langmuir*, **10**, 4681–4687.

Hansen, H.C.B. and Koch, C.B. (1995) Synthesis and characterization of pyroaurite. *Applied Clay Science*, **10**, 5–19.

Hernandez-Moreno, M.J., Ulibarri, M.A., Rendon, J.L. and Serna, C.J. (1985) IR characteristics of hydrotalcite-like compounds. *Physics and Chemistry of Minerals*, **12**, 34–38.

Kannan, S. and Swamy, C.S. (1997) Effect of trivalent cation on the physicochemical properties of cobalt containing anionic clays. *Journal of Materials Science*, **32**, 1623–1630.

Klug, H.P. and Alexander, L.E. (1974) *X-ray Diffraction Procedures*. John Wiley and Sons Inc., New York, 996 pp.

Koch, C.B. (1998) Structures and properties of anionic clay minerals. *Hyperfine Interactions*, **117**, 131–157.

Kumbhar, P.S., Sanchez-Valente, J., Millet, J.M. and Figueras, F. (2000) Mg-Fe hydrotalcite as a catalyst for the reduction of aromatic nitro compounds with hydrazine hydrate. *Journal of Catalysis*, **191**, 467–473.

Łasocha, W. and Lewiński, K. (1994) PROSZKI – a System of Programs for Powder Diffraction Data Analysis. *Journal of Applied Crystallography*, **27**, 437–438.

Miyata, S. (1975) The syntheses of hydrotalcite-like compounds and their structures and physico-chemical properties – I: The systems Mg^{2+}–Al^{3+}–NO_3^-, Mg^{2+}–Al^{3+}–Cl^-, Mg^{2+}–Al^{3+}–ClO_4^-, Ni^{2+}–Al^{3+}–Cl^- and Zn^{2+}–Al^{3+}–Cl^-. *Clays and Clay Minerals*, **23**, 369–375.

Rajamathi, M., Thomas, G.S. and Kamath, P.V. (2001) The many ways of making anionic clays. *Proceedings of the Indian Academy of Sciences – Chemical Sciences*, **113**, 671–680.

Ramos-Gallardo, A. and Vegas, A. (1996) The cation array in aluminum oxides, hydroxides and oxihydroxides. *Zeitschrift für Kristallographie*, **211**, 299–303.

Schwertmann, U. and Cornell, R.M. (1991) *Iron Oxides in the Laboratory: Preparation and Characterization*. Verlag Chemie, Weinheim, Germany, 188 pp.

Serna, C.J., Rendon, J.L. and Iglesias, J.E. (1982) Crystal-chemical study of layered $[Al_2Li(OH)_6]^+X^-{\cdot}nH_2O$. *Clays and Clay Minerals*, **30**, 180–184.

Sissoko, I., Iyagba, E.T., Sahai, R. and Biloen, P. (1985) Anion

https://doi.org/10.1346/CCMN.2005.0530103 Published online by Cambridge University Press

intercalation and exchange in $Al(OH)_3$-derived compounds. *Journal of Solid State Chemistry*, **60**, 283–288.

Taylor, H.F.W. (1969) Segregation and cation-ordering in sjögrenite and pyroaurite. *Mineralogical Magazine*, **37**, 338–342.

Twu, J. and Dutta, P.K. (1989) Structure and reactivity of oxovanadate anions in layered lithium aluminate materials. *Journal of Physical Chemistry*, **93**, 7863–7868.

(*Received 9 April 2002; revised 8 October 2004; Ms. 646; A.E. James E. Amonette*)

https://doi.org/10.1346/CCMN.2005.0530103 Published online by Cambridge University Press